AFRL-PR-WP-TP-2006-229

PULSED LASER DEPOSITION OF YBCO COATED CONDUCTOR USING Y_2O_3 AS THE SEED AND CAP LAYER

P.N. Barnes, R.M. Nekkanti, T.J. Haugan, T.A. Campbell, N.A. Yust, and J.M. Evans

MARCH 2004

Approved for public release; distribution is unlimited.

STINFO COPY

PROPULSION DIRECTORATE
AIR FORCE RESEARCH LABORATORY
AIR FORCE MATERIEL COMMAND
WRIGHT-PATTERSON AIR FORCE BASE, OH 45433-7251

REPORT DOCUMENTATION PAGE

Form Approved
OMB No. 0704-0188

1. REPORT DATE *(DD-MM-YY)*	2. REPORT TYPE	3. DATES COVERED *(From - To)*
March 2003	Journal article postprint	03/10/2003 – 03/10/2004

4. TITLE AND SUBTITLE
PULSED LASER DEPOSITION OF YBCO COATED CONDUCTOR USING Y_2O_3 AS THE SEED AND CAP LAYER

5a. CONTRACT NUMBER
In-House

5b. GRANT NUMBER

5c. PROGRAM ELEMENT NUMBER
61102F/62203F

6. AUTHOR(S)
P.N. Barnes, R.M. Nekkanti, T.J. Haugan, T.A. Campbell, N.A. Yust, and J.M. Evans (Power Generation Branch (AFRL/PRPG), Power Division)

5d. PROJECT NUMBER
3145

5e. TASK NUMBER
32

5f. WORK UNIT NUMBER
31453229

7. PERFORMING ORGANIZATION NAME(S) AND ADDRESS(ES)
Power Generation Branch (AFRL/PRPG), Power Division
Propulsion Directorate
Air Force Materiel Command, Air Force Research Laboratory
Wright-Patterson AFB, OH 45433-7251

8. PERFORMING ORGANIZATION REPORT NUMBER
AFRL-PR-WP-TP-2006-229

9. SPONSORING/MONITORING AGENCY NAME(S) AND ADDRESS(ES)
Propulsion Directorate
Air Force Research Laboratory
Air Force Materiel Command
Wright-Patterson AFB, OH 45433-7251

10. SPONSORING/MONITORING AGENCY ACRONYM(S)
AFRL-PR-WP

11. SPONSORING/MONITORING AGENCY REPORT NUMBER(S)
AFRL-PR-WP-TP-2006-229

12. DISTRIBUTION/AVAILABILITY STATEMENT
Approved for public release; distribution is unlimited.

13. SUPPLEMENTARY NOTES
Published in *Superconductor Science and Technology*, 17 (2004) 957-962. PAO Case number ASC-04-0964, April 7, 2004. This is a work of the United States Government and is not subject to copyright protection in the United States.

14. ABSTRACT
Although a variety of buffer layers have been routinely reported, a standard architecture commonly used for the $YBa_2Cu_3O_{7-x}$ (YBCO) coated conductor is YBCO/CeO_2/YSZ/CeO_2/substrate or YBCO/CeO_2/YSZ/Y_2O_3/substrate where ceria is typically the cap layer. CeO_2 is generally used as only a seed (or cap layer) since cracking within the film occurs in thicker CeO_2 layers due to the stress of lattice mismatching. Y_2O_3 has been proposed as a seed and as a cap layer but usually not for both in a given architecture, especially with all layers deposited in situ. Yttrium oxide films grown on nickel by electron beam evaporation processes were found to be dense and crack free with good epitaxy. In this report, pulsed laser deposition (PLD) of Y_2O_3 is given where Y_2O_3 serves as both the seed and cap layer in the YBCO architecture. A comparison to PLD CeO_2 is provided. Deposited layers of the YBCO coated conductor are also grown by laser ablation. Initial deposition resulted in specimens on textured Ni substrates with current densities of more than 1 MA cm^{-2} at 77 K, self-field.

15. SUBJECT TERMS
pulsed laser deposition, YBCO, superconductor, seed and cap layer

16. SECURITY CLASSIFICATION OF:			17. LIMITATION OF ABSTRACT:	18. NUMBER OF PAGES	19a. NAME OF RESPONSIBLE PERSON (Monitor)
a. REPORT	b. ABSTRACT	c. THIS PAGE			Dr. Paul N. Barnes
Unclassified	Unclassified	Unclassified	SAR	12	19b. TELEPHONE NUMBER *(Include Area Code)* (937) 255-6241

INSTITUTE OF PHYSICS PUBLISHING SUPERCONDUCTOR SCIENCE AND TECHNOLOGY
Supercond. Sci. Technol. 17 (2004) 957–962 PII: S0953-2048(04)77888-4

Pulsed laser deposition of YBCO coated conductor using Y_2O_3 as the seed and cap layer

P N Barnes[1], R M Nekkanti, T J Haugan, T A Campbell, N A Yust and J M Evans

Propulsion Directorate, Air Force Research Laboratory, WPAFB, OH 45433, USA

E-mail: paul.barnes@wpafb.af.mil

Received 10 March 2004
Published 4 June 2004
Online at stacks.iop.org/SUST/17/957
doi:10.1088/0953-2048/17/8/001

Abstract

Although a variety of buffer layers have been routinely reported, a standard architecture commonly used for the $YBa_2Cu_3O_{7-x}$ (YBCO) coated conductor is YBCO/CeO_2/YSZ/CeO_2/substrate or YBCO/CeO_2/YSZ/Y_2O_3/substrate where ceria is typically the cap layer. CeO_2 is generally used as only a seed (or cap layer) since cracking within the film occurs in thicker CeO_2 layers due to the stress of lattice mismatching. Y_2O_3 has been proposed as a seed and as a cap layer but usually not for both in a given architecture, especially with all layers deposited *in situ*. Yttrium oxide films grown on nickel by electron beam evaporation processes were found to be dense and crack free with good epitaxy. In this report, pulsed laser deposition (PLD) of Y_2O_3 is given where Y_2O_3 serves as both the seed and cap layer in the YBCO architecture. A comparison to PLD CeO_2 is provided. Deposited layers of the YBCO coated conductor are also grown by laser ablation. Initial deposition resulted in specimens on textured Ni substrates with current densities of more than 1 MA cm^{-2} at 77 K, self-field.

(Some figures in this article are in colour only in the electronic version)

1. Introduction

In high temperature superconducting (HTS) wire fabrication, $YBa_2Cu_3O_{7-\delta}$ (YBCO) superconductors are generally incorporated using coated conductor technology. To achieve the necessary bi-axial alignment, YBCO coated conductors are primarily made using the ion beam assisted deposition (IBAD), rolling assisted bi-axially textured substrate (RABiTS), or inclined substrate deposition (ISD) processes [1–5]. The RABiTS or textured substrate approach generally uses Ni alloys for the substrate which tend to be mechanically robust and as non-magnetic as possible, and allow high grain alignment [6, 7]. Different combinations of buffer layers are employed to transfer the cube texture in the metallic substrate to the subsequent YBCO layer providing proper epitaxial transfer while ensuring an adequate diffusion barrier. Primary considerations for the buffering stack must include proper matching to the adjacent crystalline lattice and thermal expansion coefficient as well as being chemically compatible and easily deposited.

Textured metallic substrate based YBCO coated conductors with the YBCO/CeO_2/YSZ/CeO_2/Ni-alloy architecture, YSZ = Zr(~8% Y)O_2, yttrium stabilized zirconium, have already demonstrated excellent performance with current densities greater than 10^6 A cm^{-2} in the superconducting layer [8]. With this architecture, the CeO_2 seed layer can effectively minimize the formation of NiO during the initial deposition on the substrate while the CeO_2 cap layer provides good lattice matching for the subsequent YBCO layer. The intermediate YSZ layer serves as an oxygen and nickel diffusion barrier. The CeO_2 cap layer on YSZ also provides chemical compatibility by suppressing the growth of $BaZrO_3$ which may occur at a YSZ/YBCO interface, causing degraded critical currents in the

[1] Address for correspondence: AFRL/PRPG, Bldg 450, 2645 Fifth Street, WPAFB, OH 45433-7919, USA.

Table 1. Comparison of lattice parameters and thermal expansion coefficients for ceria and yttria.

Lattice matching				
Buffer layer	Pseudo-cubic lattice parameter	Relative mismatch		
		YBCO (%)	Ni (%)	YSZ (%)
CeO_2	3.830 $[a/2^{0.5}]$	0.24	8.09	6.14
Y_2O_3	3.750 $[a/(2 \times 2^{0.5})]$	−1.89	6.22	4.03
Thermal expansion coefficient (TEC) matching				
Buffer layer	TEC value ($°C^{-1}$)	Relative TEC mismatch		
		YBCO (%)	Ni (%)	
CeO_2	9.5×10^{-6}	−14	−29	
Y_2O_3	7.7×10^{-6}	−30	−43	

YBCO. Even so, the CeO_2 and YBCO layers may sometimes interact, resulting in the formation of $BaCeO_3$ [9]. The reaction is especially relevant at temperatures greater than 790 °C. The resulting barium cerate is not lattice matched with the YBCO and thereby degrades its superconducting properties. However, in general, the CeO_2 cap layer has been shown to be compatible with the growth of epitaxial YBCO using most YBCO deposition techniques. As either the seed or cap layer, the CeO_2 layer must remain quite thin or cracks will develop in the thicker films due to mismatching with the adjacent lattices. A University of Houston Group uses a ~3–8% Sm doping of CeO_2 for thicker single buffer layers by photo-assisted MOCVD [10].

The present work explores an alternative approach by using yttrium oxide, Y_2O_3, as both a seed and cap layer replacement for CeO_2. Y_2O_3 is more recently being used as the seed layer in the YBCO coated conductor architecture, but generally not as the cap layer. The use of yttria allows less sensitivity to thickness by alleviating the potential cracking problems although CeO_2 is still preferred for the cap layer. A comparison of the lattice parameters and thermal expansion coefficients is given in table 1. From these data, Y_2O_3 has a better lattice match with both Ni and YSZ, indicating a better choice than CeO_2 for the seed layer. However, for the cap layer, CeO_2 has an excellent lattice match with YBCO, whereas yttrium oxide has the better lattice match with YSZ. Both are fairly comparable and compatible, though Y_2O_3 on the other hand has good chemical compatibility with YBCO and its lattice misfit with YBCO is not that great. These factors indicate Y_2O_3 may also perform well as a cap layer.

The growth of thicker Y_2O_3 buffers layers is present in the literature [11–13]. There are successful reports of the deposition of thick biaxially textured yttria layers on textured nickel by electron beam evaporation [11]. Ichinose *et al* [12] have described the process-related crystalline alignment and microstructure of Y_2O_3 buffer layers deposited under various deposition conditions by e-beam evaporation. Paranthaman *et al* have deposited other buffer layers by sputtering on top of the yttrium oxide followed by pulsed laser deposition of the YBCO layer which resulted in high current densities ($J_c \sim 1.8 \times 10^6$ A cm^{-2}) [12]. The present work uses Y_2O_3 by pulsed laser deposition (PLD) in lieu of CeO_2 as both the seed and cap layer. Limited experiments were also conducted using Y_2O_3 as a single buffer layer over nickel to evaluate its performance. All layers, including YSZ and YBCO, are deposited in the same PLD chamber *in situ*.

2. Experimental details

PLD was used to deposit all oxide layers: CeO_2, Y_2O_3, YSZ, and YBCO. A Neocera chamber was used in conjunction with a Lambda Physik excimer laser, model LPX 305i, operating at the KrF wavelength of 248 nm. The laser energy was set at 625 mJ for all depositions. With losses associated with optics and beam shaping, a final laser energy of ~2.5 J cm^{-2} was applied to an on target spot size of ~4.6 mm^2. The deposition chamber included a multiple target rotator allowing all oxide depositions for the YBCO coated conductor specimens to be deposited in the same chamber *in situ*. On select samples requiring contacts for characterization, a Ag layer of ~3 μm was applied by dc magnetron sputtering.

The background pressure of the PLD chamber was less than 10^{-6} Torr. Textured nickel substrates were obtained from Oxford Instruments—the generally used processing details have been presented elsewhere [14]. The particular substrates used in this investigation had an in-plane alignment of 6.7°–7.2° FWHM and out-of-plane alignment of 8.4°. The Ni substrates were mounted on the chamber's 2″ diameter substrate heater. Prior to deposition, substrates were heated from room temperature to 750 °C in a 180 mTorr atmosphere of forming gas, Ar + 5% H_2 gas mixture, to prevent oxidation of the nickel substrate. Specimens were fabricated to different stages in the YBCO/CeO_2/YSZ/CeO_2/Ni and YBCO/Y_2O_3/YSZ/Y_2O_3/Ni architecture. This allowed for a study of the texture, smoothness, and microstructure of each of the deposited layers and the development of the stack.

The Y_2O_3 (or CeO_2) seed layer was deposited in the Ar + H_2 forming gas mixture for 3 min at a 4 Hz laser repetition rate. The gas fill in the chamber was then evacuated and the chamber lowered to the base pressure of 10^{-6} Torr. The Y_2O_3 (or CeO_2) deposition was continued for an additional 1.5 min in these conditions. Oxygen gas was then introduced into the chamber. After stabilizing the pressure at 1.5 mTorr, the Y_2O_3 (or CeO_2) layer was further deposited for 2 min. Deposition times can be increased or decreased to change the thicknesses of the layers. The temperature was then increased from 750 to 780 °C, and the YSZ buffer layer was deposited for 20 min in the current oxygen atmosphere. For the YSZ deposition, the base laser energy was increased to 650 mJ and the repetition rate to 10 Hz. A cap layer of Y_2O_3 (or CeO_2) was deposited at the original laser energy of 625 mJ and repetition rate of 4 Hz for 2 min. After deposition of the final buffer layer, the oxygen pressure was subsequently increased to 300 mTorr and the superconducting YBCO layer was then deposited on the buffer layers. It is not suggested that these are the optimal conditions for PLD of the various layers, but are the ones used in this investigation [15]. Post-oxygenation of the films was conducted *in situ* by lowering the temperature to 500 °C and raising the oxygen pressure to 700 Torr. After 0.5 h, the heater was shut off.

The as-deposited films were analysed by a variety of characterizations. A Rigaku x-ray diffractometer was used to perform two-theta scans. To study the crystalline alignment of the substrate, buffer layers and superconductor film, omega,

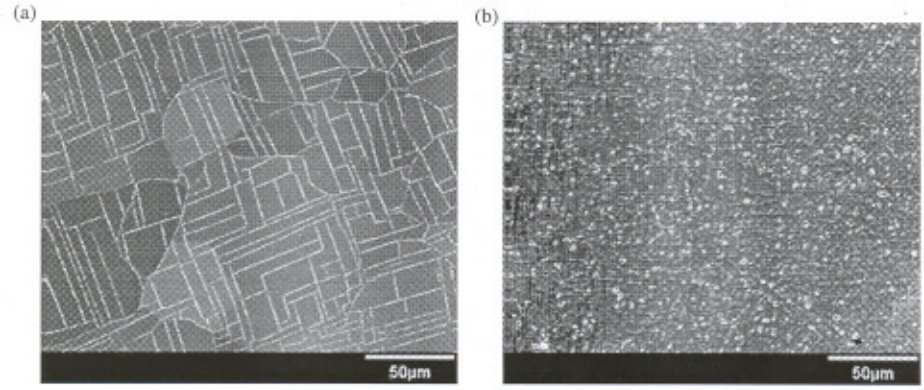

Figure 1. Planar view SEM micrographs for the YBCO/CeO_2/YSZ/CeO_2/Ni architecture at intermediate stages when using a thicker PLD CeO_2 seed layer. (a) Cracks in the thicker CeO_2 seed layer are apparent, but the grain to grain misorientation indicates excellent texture in the nickel substrate. (b) The YBCO layer displays some cracks on the surface which probably emanate from the CeO_2 layer.

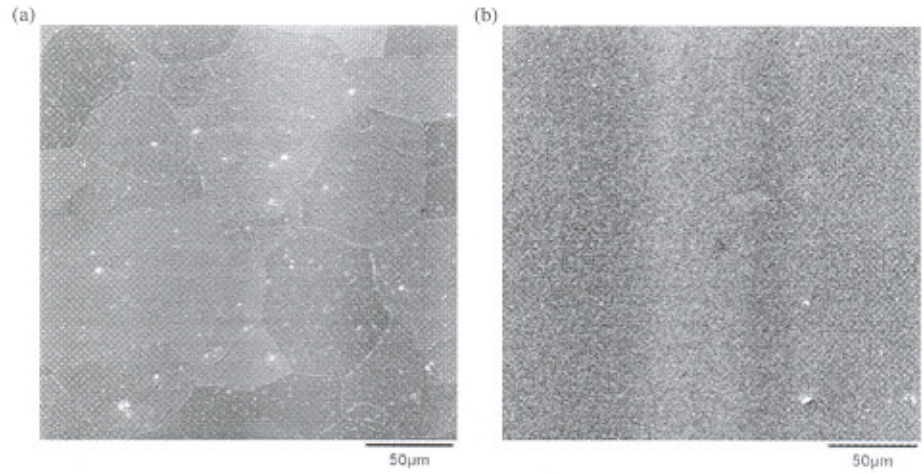

Figure 2. Planar view SEM micrographs for the YBCO/Y_2O_3/YSZ/Y_2O_3/Ni architecture at intermediate stages. (a) The surface of the Y_2O_3 seed layer is relatively smooth and uniform overall. (b) The YSZ buffer layer over the Y_2O_3 seed layer is uniform but rougher compared to the initial Y_2O_3 layer.

phi and psi scans were collected using a Philips MRD with four-circle diffractometry. The microstructure of the various films was evaluated under scanning electron microscopy (SEM) using a Leica SEM microscope and field emission gun for the surface roughness and film structure morphology. A Digital Instruments atomic force microscope (AFM) was used to more fully characterize the roughness of the buffer layers. The quality of YBCO was additionally evaluated by ac susceptibility measurements to determine the critical transition temperatures (T_c s). Electrical property characterizations of the samples' full width, 5 mm, were made using a standard four-probe technique with a 1 μV cm^{-1} criterion to determine the critical current (I_c) as well as the resistive T_c. The thicknesses of the films were determined by etching the YBCO at an edge and measuring step height using a profilometer.

3. Results and discussion

Scanning electron micrographs (SEMs) for the YBCO/CeO_2/YSZ/CeO_2/Ni (using a thicker ceria seed layer) and YBCO/Y_2O_3/YSZ/Y_2O_3/Ni architecture are given in figures 1 and 2, respectively. Although thickness variations of layers were performed in this study as outlined in this section, the standard thicknesses used for the two architectures are a CeO_2 seed layer of 80 nm, a Y_2O_3 seed layer of 130 nm, a YSZ layer of 360 nm, a CeO_2 cap layer of 40 nm, a Y_2O_3 cap layer of 40 nm and a YBCO layer of 300 nm. Typically, CeO_2 seed layers $<\sim$100 nm thick do not crack. As the seed layer gets thicker cracking increases as evident in figure 1(a) for a 100 nm thick CeO_2 layer. In the figure, the low misorientation in the nickel substrate can be gauged from the cracking pattern in the CeO_2 on adjacent Ni grains. Cracking is not the case with a Y_2O_3 layer, figure 2(a), which tends not to crack even at a few hundred nm thick, as determined in this study and elsewhere. Thicker ceria seed layers induced cracking although yttria layers did not crack even as the thickness increased. Some cracking is evident in the YBCO layer per figure 1(b) (left-hand side of SEM) which probably emanates from the underlying cracks in the initial CeO_2 layer. Figure 2(b) is an SEM of the YSZ layer grown on top of a Y_2O_3 seed layer. At this point the

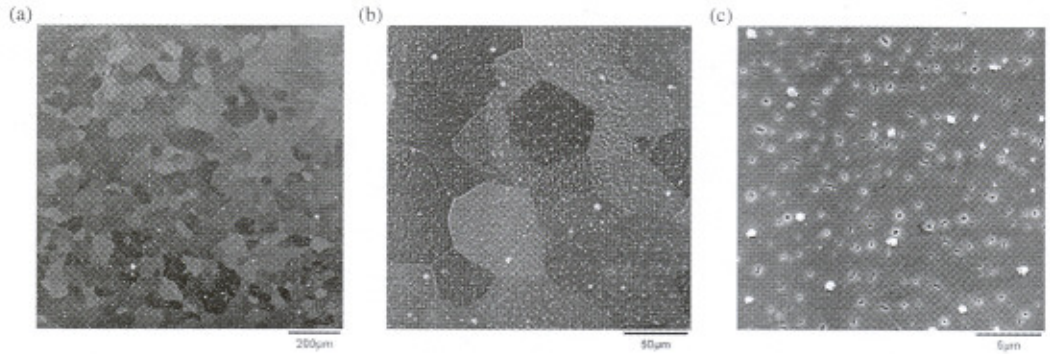

Figure 3. SEM micrographs of the superconducting YBCO layer at different magnifications when using the YBCO/Y_2O_3/YSZ/Y_2O_3/Ni architecture.

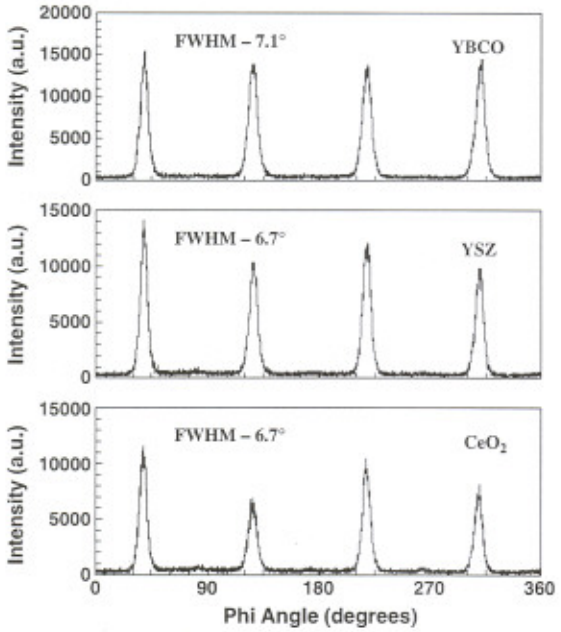

Figure 4. Phi scans for the YBCO/CeO_2/YSZ/CeO_2/Ni architecture at intermediate stages. The CeO_2 seed layer is used and the Ni substrate is of the same lot as used for the sample phi scans in figure 5.

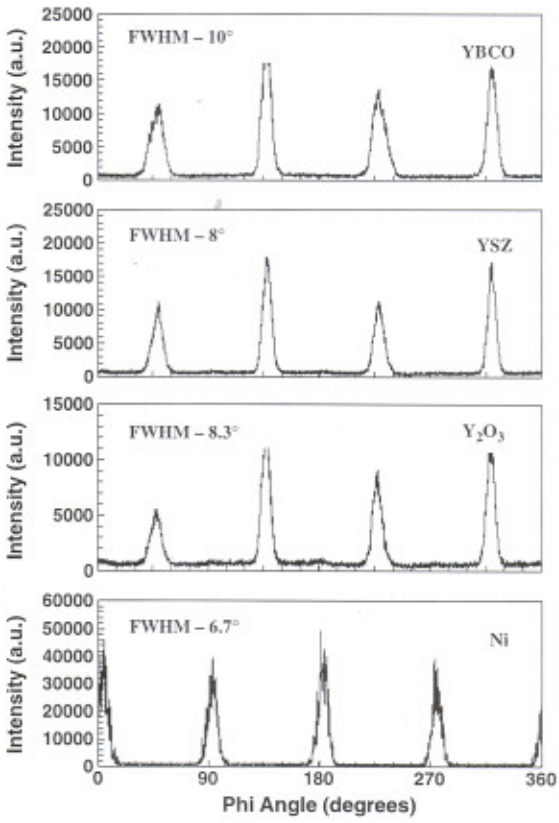

Figure 5. Phi scans for the YBCO/Y_2O_3/YSZ/Y_2O_3/Ni architecture at intermediate stages. The Y_2O_3 seed layer is used in the phi scans.

underlying Ni grain boundaries are not evident in the SEM but are probably imprinted in the YSZ layer [16]. This is clear in figure 3 which displays different magnifications of the YBCO layer on the Y_2O_3/YSZ/Y_2O_3/Ni buffered tape architecture where they are apparent.

To examine the epitaxial growth of the successive layers and determine the transfer of the underlying textured alignment, a series of XRD scans was taken. X-ray theta–two-theta scans on the intermediate buffer layers of both architectures showed sharp (00*l*) peaks indicating excellent *c*-axis texture in buffer layers which was carried over to the superconducting YBCO layer. Phi scans of the different oxide layers on nickel indicate excellent in-plane alignment of the various layers although better for the ceria architecture using the present deposition conditions. Figure 4 gives the different phi scans of the YBCO/CeO_2/YSZ/CeO_2/Ni architecture for the given deposition conditions. Figure 5 displays phi scans of the YBCO/Y_2O_3/YSZ/Y_2O_3/Ni architecture which includes the phi scan of the Ni substrate; this phi scan is not duplicated in figure 4 but is also applicable for those figures. With a starting Ni phi scan full width at half maximum (FWHM) of 6.7°, the subsequent phi scans are for the ceria architecture CeO_2 seed = 6.7°, YSZ = 6.7° and YBCO = 7.1°, and for the yttria architecture Y_2O_3 seed = 8.0°, YSZ = 8.3° and YBCO = 10°. In the present work, a larger degradation in

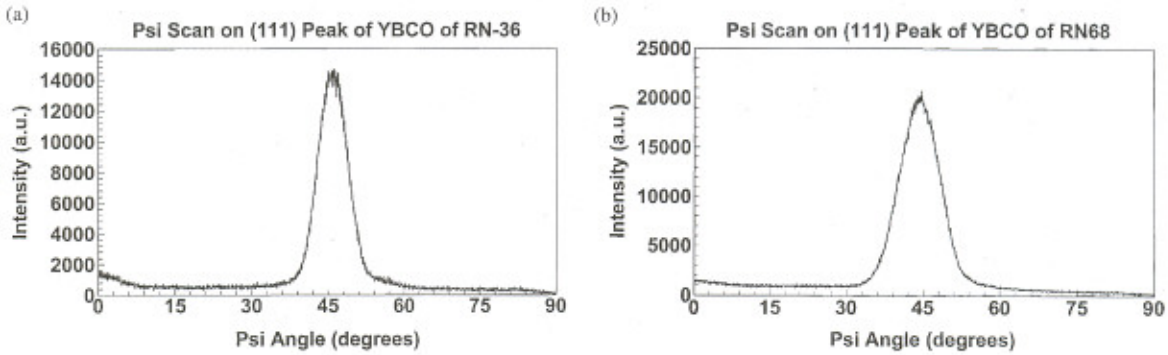

Figure 6. Psi scan on the (111) peak of the YBCO layer of specimen for (a) the YBCO/CeO_2/YSZ/CeO_2/Ni architecture, and (b) the YBCO/Y_2O_3/YSZ/Y_2O_3/Ni architecture.

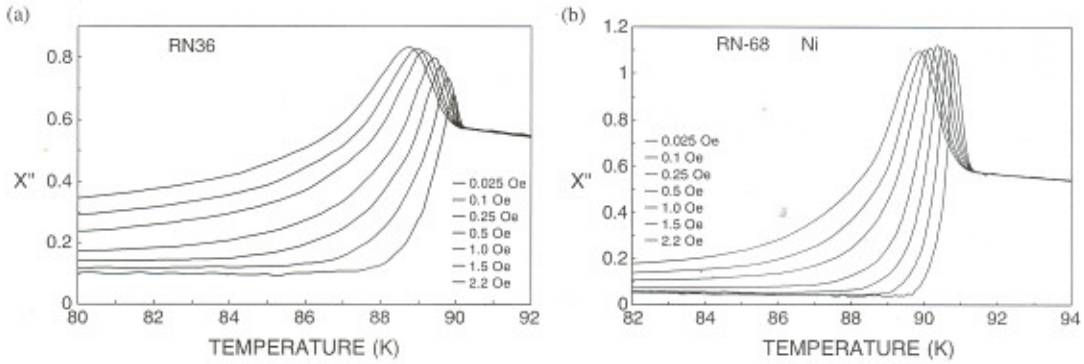

Figure 7. Ac susceptibility data indicating the onset T_c for (a) the YBCO/CeO_2/YSZ/CeO_2/Ni architecture, and (b) the YBCO/Y_2O_3/YSZ/Y_2O_3/Ni architecture. The different curves result from the different applied fields listed in the legend—the field increases from right to left.

epitaxial transfer occurred for the Y_2O_3 layer; FWHMs of the Y_2O_3, YSZ and YBCO layers were increased $>1°$, as opposed to the FWHMs of CeO_2 and related layers which had $<1°$ variation. Even so, both layer structures were acceptable from this standpoint. Psi scans of the final YBCO layer are given in figure 6 for the different architectures. Both indicate acceptable FWHMs although the architecture using the CeO_2 seed and cap layers is again slightly better than the architecture with Y_2O_3 layers.

Preliminary experiments resulted in specimens with current densities of more than 1 MA cm^{-2} at 77 K in self-field for both architectures. The I–V plot of the current measured in a specimen using the YBCO/Y_2O_3/YSZ/Y_2O_3/Ni architecture indicated a 5 mm wide sample carried a critical current (I_c) of 18 A at liquid nitrogen temperature which is equivalent to a J_c of 1.2 MA cm^{-2}. A 5 mm wide specimen measured using CeO_2 as the seed and cap layer in the coated conductor architecture carried an I_c of 15 A across it equivalent to a J_c of 1.0 MA cm^{-2}. Ac susceptibility data of the same samples measured for J_c are given in figure 7 in which χ'', the imaginary loss component, is plotted versus temperature. The data were obtained for different applied magnetic fields as indicated in the figure. The onset T_c obtained for the YBCO/Y_2O_3/YSZ/Y_2O_3/Ni architecture is slightly higher than that for the YBCO/CeO_2/YSZ/CeO_2/Ni architecture. The spread of the magnetic field lines in the ac susceptibility data indicate a generally good film [17]. This preferred value for the use of the Y_2O_3 seed and cap layer is in agreement with the transport measurements but differs from the XRD given previously. Even so, values are fairly similar in each case.

The SEM micrographs of the superconducting YBCO layer with yttria cap and seed layers, given previously in figure 3, indicate the surface is relatively smooth with uniform coverage and without too many overgrowths. An AFM image of the YBCO layer using the YBCO/Y_2O_3/YSZ/Y_2O_3/Ni architecture is given in figure 8, although from another sample grown under the same conditions as the sample used for figure 3. The outgrowths, or particulates on the surface, are evident here as the dark peaks. The AFM scan on this specimen gives the following RMS roughness over a 50 μm × 50 μm area: R_q = 62.6 nm including the outgrowths and R_q = 36.765 nm over the same area if outgrowths are excluded. This can be compared to the roughness of the YSZ layer, which is R_q = 35.1 nm, and the Y_2O_3 seed layer, being R_q = 18.8 nm. The final surface increases in roughness with the additional layers and greater thickness as is expected.

4. Conclusions

Yttrium oxide was successfully incorporated as both a seed and a cap layer in fabricating YBCO coated conductor specimens on a textured nickel substrate in a single chamber using pulsed laser deposition. Its usefulness is comparable to the YBCO/CeO_2/YSZ/CeO_2/Ni architecture where CeO_2 is used

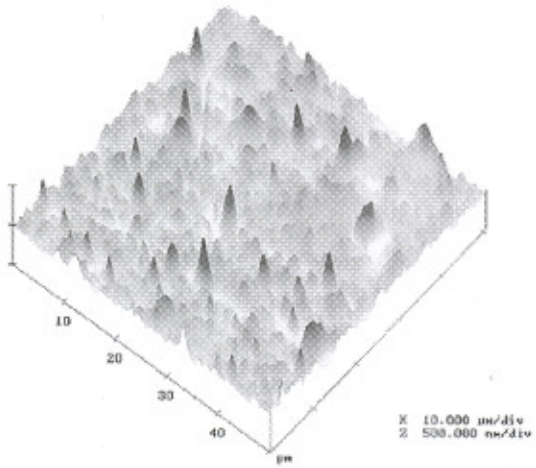

Figure 8. AFM showing the surface morphology and roughness of the YBCO layer. Note the planar scale is 10 μm per division and the vertical scale is 500 nm per division.

instead. This is more advantageous to pulsed laser deposition when a limited number of targets can be placed in the target holder for *in situ* deposition. Good epitaxy was observed in all the deposited layers of the YBCO/Y_2O_3/YSZ/Y_2O_3/Ni as well as the YBCO/CeO_2/YSZ/CeO_2/Ni architectures leading to a high onset T_c (~90–91 K) and self-field J_c of more than 1 MA cm^{-2} on multiple samples created under similar conditions. The microstructure of the yttrium oxide and the superconducting YBCO layers were dense and crack free with uniform coverage across the sample in comparison to the CeO_2 and YBCO layers in the CeO_2 structures.

Acknowledgment

Ac susceptibility data were provided by I Maartense of the Air Force Research Laboratory.

References

[1] Selvamanickam V, Lee H G, Li Y, Xiong X, Qiao Y, Reeves J, Xie Y, Knoll A and Lenseth K 2003 *Physica* C **392–396** 859–62
[2] Verebelyi D T *et al* 2003 *Supercond. Sci. Technol.* **16** L19–22
[3] Groves J R *et al* 2002 *Physica* C **382** 43–7
[4] Goyal A *et al* 2001 *Physica* C **357–360** 903–13
[5] Balachandran U, Ma B, Li M, Fisher B L, Koritala R E, Miller D J and Dorris S E 2003 *Physica* C **392–396** 806–14
[6] Nekkanti R, Seetharaman V, Brunke L, Maartense I, Dempsey D, Kozlowski G, Tomich D, Biggers R, Peterson T and Barnes P 2001 *IEEE Trans. Appl. Supercond.* **11** 3321–4
[7] Paranthaman M, List F A, Sathyamurthy S, Aytug T, Cook S, Goyal A and Kroeger D M 2003 *ORNL Technical Report* HTSPC-14 *ORNL Superconducting Technology Program for Electric Power Systems, Annual Report for FY 2002* ed W S Koncinski pp 1-11–12
[8] Yang C Y, Babcock S E, Goyal A, Paranthaman M, List F A, Norton D P, Kroger D M and Ichinose A 1998 *Physica* C **307** 87–98
[9] Holesinger T G, Foltyn S R, Arendt P N, Jia Q, Dowden P C, DePaula R F and Groves J R 2001 *IEEE Trans. Appl. Supercond.* **11** 3359–64
[10] Ignatiev A, Zhang X, Zeng J and Molodyk A 2003 MOCVD routes to the development of HTS coated conductor wire *105th American Ceramic Society Mtg (Nashville, TN)*
[11] Paranthaman M, Lee D F, Goyal A, Specht E D, Martin P M, Cui X, Mathis J E, Feenstra R, Christen D K and Kroeger D M 1999 *Supercond. Sci. Technol.* **12** 319–25
[12] Ichinose A, Yang C, Larbalestier D, Babcock S, Kikuchi A, Tachikawa K and Akita S 1999 *Physica* C **324** 113–22
[13] Lee D F *et al* 1999 *Japan. J. Appl. Phys.* **38** L178–80
[14] Marken K 2002 *Development of Metal Strip for RABiTS in Superconductivity for Electric Systems Meeting Proceedings* (DOE/EE-SES/JUL2002-CD compiled by Energetics, Inc.)
[15] Haugan T, Barnes P, Maartense I, Brunke L and Murphy J 2003 *Physica* C **397** 47–57
[16] Feldmann D M *et al* 2000 *Appl. Phys. Lett.* **77** 2906–8
[17] Barnes P N, Maartense I, Peterson T L, Haugan T J, Westerfield A L, Brunke L B, Sathiraju S and Tolliver J C 2004 *Mat. Res. Soc. Symp. Proc.* EXS-3 EE6.4.1-3